per genotype) using in some cases second RNAi transformants to control for transgenic insertion effects and second independent RNAi hairpins to target a different region of the gene (Table S2). After repeated screening we identified 498 genes that passed the more stringent Z-score of 3 (Fig. 1E and Table S2) indicating that these hits exhibit a death score of 3 standard deviations from the mean. Using gene ontology (GO) annotations, our candidate hits were classified according to their predicted biological processes (BP), molecular functions (MF), and cellular components (CC). Of the classified genes, those involved in signaling, ion transporter activity, metabolism and mitochondrial structure, development and morphogenesis, transcriptional regulation, or nucleic acid binding were highly represented among the entire data set (Fig. S2 and Table S4A). To remove any artificial bias in the gene list created by the ad-hoc Z score cut-off >3, we performed a Gene Set Analysis (GSA) to confirm enrichment of selected GO terms (Table S4B). In addition, 121 candidate heart genes had no annotated function by GO. Using panther (http://www.pantherdb.org/) we were able to functionally annotate 116 of these genes (Table S4C).

Given that the RNAi library screened is known to generate a level of false negative phenotypes due to inefficient targeting of genes to levels required to reveal phenotypes (Dietzl et al., 2007), and based on the assumption that our candidate heart hits perform some of their functions in protein complexes, we next identified first degree binding partners (Table S4D). Using this list of primary heart hits and their binding partners, we performed fly KEGG pathway analyses. Moreover, we included developmental lethal hits to generate a global interaction network. KEGG analyses showed enrichment of multiple pathways, such as mTOR signaling and PI3K/AKT, amino acid metabolism, JAK-STAT signaling, ErbB signaling, the Wnt, Notch, hedgehog, or TGFβ pathways, protein degradation, VEGF signaling, DNA repair, and Calcium homeostasis (Table S3 and Table S4E). Besides the identification of multiple known genes, our screen has also revealed hundreds of candidate genes and pathways that have not been previously associated with heart function.

A global view of heart function

To extend our *Drosophila* results to mammalian systems we used the power of data-mining and bioinformatics at a global systems level. Potential mouse and human orthologues of our candidate heart screen hits were evaluated for GO enrichment. The GO analyses of the human and mouse orthologues showed marked enrichment of genes involved in PIP3 and calcium signaling, ion transporter activity, metabolism, development, fatty acid metabolism, or muscle contraction (Table S4F). We next performed KEGG pathway as well as Broad Institute C2 gene set analysis on the mouse and human orthologues and their first degree binding partners. Based on the mammalian KEGG (Table S4E) and C2 (Table S4G) analyses, we found significant enrichment for gene sets involved in signaling, metabolism, ion channels, inflammation, aging, and transcription.

To generate a network map that includes our functional data in *Drosophila*, their human and mouse orthologues, and first degree binding partners, KEGG pathways from *Drosophila*, mouse and human were combined with relevant gene sets from the Broad Institute C2 annotations (Tables S4). A combined systems map and the interactions between the individual genes in the indicated nodes are shown in Fig. 2 and Table S4H. A systems map using only direct screening hits was also generated, yielding a comparable network map (Table S3). Importantly, using this network approach we identified multiple pathways known to play key roles in heart function and cardiovascular disease. For instance, we found significant enrichment in NFAT transcription, AKT activation and PI3K signaling, calcium signaling and muscle contraction, GPCR- and cAMP signaling, ion channels and proton-transporting ATPase complexes, and transcription. We also found associations with the renin-angiotensin system, a key pathway involved in cardiovascular function in humans (Fig. 2 and Table S4H). In support

of our network approach, advanced data mining revealed that 171 of our primary fly hits and their first degree binding partners corresponded to mouse knock-outs with known cardiovascular phenotypes (Table S5). Thus, our genome-wide screen for candidate heart genes and *in silico* analyses provides a first attempt at a global road-map of essential molecular components and key pathways potentially involved in heart function and cardiac failure.

RNAi silencing of *not3* and *UBC4* result in dilated cardiomyopathy in *Drosophila*

One of the novel pathways we found in our global network analyses was the CCR4-Not complex (Fig. 2 and Table S3). Intriguingly, among the 8 members of this complex assayed, we hit the subunits not1, not3 (not3/5 in fly), not4, UBC4, and Hsp83 (Fig. 3A). In addition, the subunits not2 and CG8759 were "weak" hits (Fig. 3A). The CCR4-Not complex was first identified in yeast (Denis, 1984) and is highly conserved in evolution (Albert et al., 2000). Components of the CCR4-Not complex have not yet been associated with cardiovascular function. We therefore re-tested components of this pathway using TinCΔ4-Gal4-driven knockdown in the heart, which confirmed the phenotype (Fig. 3B). Moreover, use of a second heart driver, Hand-Gal4, which is expressed with high specificity in myocardial and pericardial cells throughout development and in the adult fly heart (Han and Olson, 2005), showed that silencing of *not1*, *not3*, and *UBC4* resulted in early death when adult flies were shifted to 29° C (Fig. 3B).

Since not3 RNAi lines gave a strong phenotype with two different UAS-RNAi lines (Fig. 3B), we focused on the CCR4-Not component not3. Cardiac specific knockdown of not3 using two different RNAi lines (Hand>not3-RNAi: progeny from Hand-Gal4 crossed to UAS-not3-RNAi) significantly increased both diastolic and systolic diameters and resulted in a marked reduction in systolic fractional shortening relative to control flies (Fig. 3C–F and supplemental video 1). Hearts with cardiac not3 knockdown also showed slight increases in heart periods (Fig. 3G), however this was not statistically significant. Fluorescent microscopy revealed that not3 RNAi lines exhibit marked myofibrillar disarray, especially in the conical chamber (Fig. 4A–D). Heart-restricted not3-RNAi-mediated knockdown was confirmed by qRT-PCR (Fig. S3). In addition, we observed transcriptional downregulation of the Sarcoplasmic/endoplasmic reticulum calcium ATPase (Serca2a, ATP2A2), myosin heavy chain (mhc, MYH7), and the potassium channel KCNQ (kcnq1, KCNQ1) (Fig. S3) involved in heart rhythm control. Cardiac-specific knockdown of not3 increased the number of flies exhibiting contractile irregularities (Fig. S3H,I), a finding similar to what is seen in response to cardiac-specific knockdown of the KCNQ K^+ channel (Fig. S3I) and what has been reported for KCNQ mutant flies (Ocorr et al, 2007). Of note, a not3 P-element mutant was developmentally lethal, exhibiting a late stage defect in embryonic heart tube organization, which could be rescued by P-element excision (Fig. S3C).

The CCR4-Not complex component UBC4 was also a major hit identified by our heart screen. Moreover, *UBC4* expression was reduced following *not3* knockdown (Fig. S3B). Hand-Gal4>UAS-*UBC4*-RNAi flies also exhibited significantly longer heart periods and showed dramatically altered diastolic and systolic diameters and reduced fractional shortening relative to control hearts (Fig. 3C–G). Fluorescent imaging again revealed severe myofibrillar disarray (Fig. 4D). that was strikingly similar to that observed in *not3* knock-down hearts. Further, we observed similar structural and functional phenotypes in *not1* cardiac-specific knock-down flies (A.C., G.N., J.P. and R.B., unpublished observation). Thus, knock-down of different components of the CCR4-Not complex result in abnormal heart structure and severely impaired cardiac function indicative of dilated cardiomyopathy.

Functional assessment of additional *Drosophila* heart hits

To extend our confirmations beyond the CCR4-Not complex, we assayed heart function in adult flies with heart-specific knock-down of four additional candidates identified in our heart screen (Fig. S3). One candidate heart gene tested was CG1216 (Mrityu), a mesoderm-expressed BTB-POZ domain containing protein (Rusconi and Challa, 2007). Cardiac knock-down of CG1216 resulted in a significant increase in systolic diameter. Another candidate heart gene is CG8933 (extradenticle), a PBX-family transcription factor. Cardiac knock-down of CG8933 resulted in increased systolic diameter and reduced fractional shortening. Cardiac knockdown of CG33261 (Trithorax-like) resulted in significantly altered diastolic and systolic diameters as well as impaired fractional shortening. Finally, knock-down of CG7371, a Vps52-domain containing protein predicted to participate in Golgi trafficking, resulted in a marked increase in heart period and affected the diastolic diameter. These data further demonstrate that our screen indeed has the capacity to identify novel factors involved in and required for normal adult heart function.

Generation of *not3* knock-out mice

We next tested whether our data on *Drosophila* can be directly translated into a mammalian species. The mouse and human not3 proteins (official gene name *cnot3*) share 60% identity with the *Drosophila not3* orthologue. Expression of human and mouse *not3* mRNA transcripts can be found in the majority of tissues analysed. Although not3 is evolutionarily conserved from yeast to mammals, essentially nothing is known about the *in vivo* role of mammalian not3. We therefore generated *not3* knock-out mice.

We disrupted the *not3* gene in murine embryonic stem (ES) cells using a targeting vector in which nucleotides encompassing exons 2 through 9 are deleted (Fig. 5A and Fig. S4A). Both $not3^{+/-}$ male and $not3^{+/-}$ female mice are viable and exhibit normal fertility. We never obtained viable $not3^{-/-}$ newborn mice indicating that loss of not3 results in embryonic lethality. We staged embryonic development but failed to recover *not3* null embryos from placental implantations (Fig. S4B,C). We therefore assayed early embryogenesis and observed that $not3^{-/-}$ blastocysts can develop. These mutant blastocysts have a normal appearance (Fig. S6D), occur at Mendelian frequencies (Fig. S4E,F), and express key markers of early embryonic differentiation at normal levels (Fig. S4G). *not3* mRNA transcripts and not3 protein were undetectable in $not3^{-/-}$ blastocysts by RT-PCR and immunostaining (Fig. S4F,G). In $not3^{+/+}$ and $not3^{-/-}$ epiblast cultures (Fig. S4H), trophoblast cells started to spread and supported the outgrowths of the inner cell mass (ICM). While the ICM of $not3^{+/+}$ blastocysts continued to grow, $not3^{-/-}$ ICM cells exhibited a severe outgrowth defect. Thus, complete loss of mouse not3 results in early embryonic death at the implantation stage.

not3 haploinsufficiency results in impaired heart function

We speculated that similar to RNAi-mediated down-regulation of not3 in *Drosophila*, *not3* haploinsufficiency might also reveal a role in mammalian heart function. In *not3* heterozygote mice, not3 expression is indeed downregulated in the heart (Fig. 5B). We failed to observe overt structural changes in the hearts of $not3^{+/-}$ mice. However, both male and female *not3* haploinsufficient mice exhibited a reduction in cardiac contractility as determined by decreased left ventricle fractional shortening and increased left ventricular diameter in systole (Fig. 5C,D).

To address whether the defects in cardiac function are intrinsic to the heart *per se* or the observed impairment of contractility was secondary due to haploinsufficiency of *not3* in other tissues, we subjected explanted hearts from wild-type and $not3^{+/-}$ littermate mice to Langendorff perfusion, assessing *ex vivo* heart function (Joza et al., 2005). When isoproterenol was used to activate β-adrenergic receptors, $not3^{+/-}$ hearts exhibited severe contractile

abnormalities as defined by impaired generation of left ventricular pressure (LVP) (Fig. 5E and Fig. S5A). Hemodynamic measurements confirmed that all functional heart parameters such as dP/dT_{max} or dP/dT_{min}, indicative of generated contractile pressure, were markedly reduced in *not3*$^{+/-}$ hearts (not shown). Moreover, when explanted hearts were electrically stimulated, *not3*$^{+/-}$ hearts exhibited a striking defect in contractility (Fig. 5F). Thus, downregulation of not3 expression in *not3* haploinsufficient mice results in an intrinsic impairment in heart function.

Yeast strains mutant for components of the CCR4-Not complex, including not3, display reduced acetylation levels of lysine residues on histone tails (*e.g.* H3K9) (Peng et al., 2008) and/or reduced trimethylation of H3K4 (Laribee et al., 2007). H3K9 acetylation and H3K4 trimethylation are indicative of transcriptionally active states of chromatin. Moreover, promoter regions of not3 target genes were shown to recruit trimethylated H3K4 in mouse ES cells (Hu et al., 2009) suggesting that not3 may regulate chromatin modifications. Our gene expression and bioinformatic analyses of mouse *not3* knockout cells revealed that histone deacetylases (HDACs) and mRNA metabolisms are localized central in gene networks (unpublished). We therefore assessed the state of histone modifications in hearts from *not3*$^{+/-}$ mice. Histone extracts of whole hearts from *not3* haploinsufficient mice showed a slight but significant reduction in active histone marks such as acetylation of H3K9 and trimethylation of H3K4 (Fig. 5G, 5H and Fig S5). H3K27 trimethylation was not changed (Fig. 5I and Fig S5). Treatment of *not3*$^{+/-}$ hearts with the HDAC inhibitor VPA restored the reduced acetylation of H3K9 and H3K4 trimethylation to that of wild type levels (Fig. 5G–I and Fig. S5). Most importantly, administration of HDAC inhibitors rescued the impairment in heart function in *not3*$^{+/-}$ mice; i.e. *ex vivo* heart functions of VPA treated mice were similar to control mice in response to both isoproterenol (Fig. 5J) and electrical stimulation (Fig. 5K). These data were confirmed using TSA, a second HDAC inhibitor (Fig. S5H,I). Taken together, *not3*$^{+/-}$ mice exhibit a spontaneous and intrinsic defect in cardiac function which can be rescued with HDAC inhibitors.

not3$^{+/-}$ mice develop severe cardiomyopathy in response to cardiac stress

We next exposed control and *not3*$^{+/-}$ littermates to chronic pressure overload by surgical constriction of the aorta (transverse aortic constriction, TAC). Three weeks after TAC, heart weight/body weight ratios (HW/BW) increased in both *not3*$^{+/+}$ and *not3*$^{+/-}$ mice, albeit this increase was significantly larger in the *not3*$^{+/-}$ mice (Fig. 6A). Cardiac hypertrophy was also seen by histology (Fig. 6D and S6A). Aortic banding of *not3*$^{+/-}$ mice resulted in severe heart failure characterized by decreased fractional shortening (Fig. 6B) and a dilation of the left ventrical as determined by echocardiography (Fig. 6C). In addition, *not3*$^{+/-}$ mice develop severe cardiac fibrosis following TAC, as shown by Masson-trichrome staining of hearts 3 weeks after TAC (Fig. 6D and Fig. S6B). Thus, *not3*$^{+/-}$ mice develop severe symptoms of heart failure in response to cardiac stress.

We next assessed whether HDAC inhibitors can also rescue stress-induced heart failure. HDAC inhibitor treatment could indeed block the augmented loss of cardiac function observed in *not3*$^{+/-}$ mice following TAC (Fig. 7A,B). *In vivo* treatment of *not3*$^{+/-}$ mice with HDAC inhibitors also blocked the exaggerated induction of heart failure markers such as ANF (Fig. S6C) and βMyhc (Fig. S6D). Moreover, treatment with an HDAC inhibitor restored the observed histone alterations in *not3*$^{+/-}$ mice to that of wild type littermates (Fig. 7C and Fig. S6E,F). Thus, not3 haploinsufficiency results in exaggerated heart failure which can be rescued by HDAC inhibition *in vivo*.

A common genomic variation in the *NOT3* promoter correlates with cardiac repolarization duration in humans

Using an *in silico* search to identify not3 target genes, we found that not3 has been shown to bind to the Kcnq1 promoter in ES cells (Hu et al., 2009). Kcnq1 encodes the α-subunit of the repolarizing voltage gated potassium channel I_{Ks}, mutations in which are the most common cause of long-QT syndrome (LQT1) in humans (Wang et al., 1996). Abnormalities of cardiac repolarization, measured as alterations in QT interval, predispose to sudden cardiac death in humans (Moss and Kass, 2005). Indeed, while sham-operated *not3*$^{+/-}$ mice exhibit a subtle reduction in cardiac Kcnq1 expression, this decrease was pronounced following TAC (Fig. 7D). Reduced Kcnq1 expression was rescued following HDAC inhibitor treatment. Also for Kcne1, the β-subunit of I_{Ks}, we observed a TAC-inducible and HDAC-sensitive defect in expression in *not3*$^{+/-}$ hearts (Fig. 7E). In fly not3-RNAi hearts, KCNQ expression is also reduced (Fig. S3D), and these flies exhibit cardiac contractile irregularities (Fig. S3H,I).

Recently two consortia have published genome-wide association studies (GWAS) for QT interval, QTSCD (Pfeufer et al., 2009) and QTGEN (Newton-Cheh et al, 2009). One of the 12 identified genomic regions contains the *NOT1* gene which we also found as a hit in our *Drosophila* screen (Fig. 3A and B). Due to the stringent requirements to achieve a genome-wide significance threshold of $p<5\times10^{-8}$ (Dudbridge and Gusnanto, 2008), many genuinely associated alleles will be missed because of both a failure to exceed this statistical threshold and the absence of functional confirmatory data for genes within loci of interest. We therefore evaluated whether common variants in and near the human *NOT3* locus are associated with alterations in QT interval. Intriguingly, SNP rs36643 (chromosome 19: 59,3 Mb), located in the promoter region ~969 base pairs upstream from the *NOT3* transcriptional start site (924 bases upstream of the TATA box), significantly associates with QT interval in the QTSCD dataset (Fig. 7F). Patients carrying the common T allele (MAF = 0.65) showed a dose-dependent increase in QT intervals (ES= +1.03±0.29 ms QT interval per copy of T-allele, $p=3.66E^{-04}$) (Fig. 7G). Of note, similar to adult *kcnq1* mutant mice (Nerbonne, 2004), we did not observe an increased QT interval in *not3* heterozygous mice (except for one mouse with arrhythmia, K.K., M.M., H.Y. and K.F. unpublished). Thus, our genome-wide screening data for death in flies can be used to identify candidate variants in humans that predispose individuals to heart disease, i.e. in the case of Not3 to arrhythmia and sudden death.

DISCUSSION

Here we present the first *in vivo* RNAi adult heart screen in *Drosophila* assaying conserved genes. Using functional imaging, we were able to observe cardiac defects in all flies with heart-specific knockdown of candidate genes evaluated to date. Our experimental approach to screen for conserved heart genes in *Drosophila* in concert with advanced bioinformatics has the potency to reveal human and mouse genes involved in heart function and heart disease. Moreover, we uncovered a plethora of additional genes, a large proportion of which had completely unknown functions until now. Future experiments are required to test whether our novel candidate genes indeed control cardiac development, regulate adult heart function, and/or influence the outcome of heart failure in response to cardiac stress.

One pathway we identified was the CCR4-Not complex. Functional heart analyses in *Drosophila* confirmed that RNAi-mediated silencing of the CCR4-Not components *not3* and *UBC4* resulted in a severe impairment of cardiac function that resembles dilated cardiomyopathy in experimental mouse models and human patients. To provide a first proof-of-principle that our fly hits can indeed have similar functions in the more complex mammalian heart, we generated knock-out mice for a component of the CCR4-Not complex. *not3* haploinsufficient mice develop spontaneous impairment of heart function and severe heart failure following aortic banding. Mechanistically, *not3* downregulation results in a defect in

active histone marks and cardiac defects observed in *not3*$^{+/-}$ mice could be rescued by treatment with HDAC inhibitors. Besides regulating transcriptionally active states of chromatin (Hu et al., 2009; Jayne et al., 2006; Laribee et al., 2007; Peng et al., 2008), the CCR4-Not complex has also been implicated in RNA deadenylation (Tucker et al., 2001) and microRNA-mediated mRNA degradation (Behm-Ansmant et al., 2006). Thus, we cannot exclude that CCR4-Not components affect additional mechanisms regulating heart function. Importantly, our work on *not3* in flies and mice has also allowed us to identify a SNP in the human *NOT3* promoter that is associated with prolonged QT intervals and sudden cardiac death in humans. Thus, large scale screens in *Drosophila* can be directly translated to mammalian species, and in combination with other genome-wide approaches, can reveal novel regulators of heart function and heart failure.

EXPERIMENTAL PROCEDURES

Detailed experimental procedures are provided in the Supplemental Data.

Fly stocks

All RNAi transgenic fly lines were obtained from the VDRC RNAi stocks (Dietzl et al., 2007). The cardiac-tissue specific TinCΔ4 12a-Gal4 was a kind gift from Manfred Frasch, (Lo and Frasch, 2001) and Hand-Gal4 was a gift from Eric Olsen (Han and Olson, 2005).

Screening system

Transgenic RNAi males were crossed to TinCΔ4 virgin females. Viable lines were then incubated at 29°C for 6 days to expose flies to temperature stress (Paternostro et al., 2001). Initially a Z score cut-off of 2 (Mean control-test)/SD was used to select RNAi lines for re-testing.

Drosophila cardiac function, morphology and gene expression

UAS-RNAi fly lines obtained from the Vienna *Drosophila* RNAi Center were crossed to Hand-Gal4 (II) driver-flies and to w^{1118} wild type control flies. Flies were assessed for heart morphology and physiology using imaging (Ocorr et al., 2007b). M-modes were generated and cardiac parameters including heart periods, diastolic and systolic diameters and fractional shortening were recorded for each group using a MatLab-based image analysis program (Fink et al., 2009). Fluorescent imaging of *Drosophila* heart tubes was performed as described (Alayari et al., 2009).

Bioinformatics analysis

For a detailed description of full bioinformatics analysis, please see supplemental experimental procedures.

Phenotyping of *not3* knockout mice

A targeting vector was constructed to replace exons 2 and 9 of the murine *not3* gene. Fractional shortening (FS) was calculated as follows: FS = [(LVEDD − LVESD)/LVEDD] × 100. For ex vivo heart studies, hearts were assayed using a Langendorff apparatus. The heart was paced electrically at 400 beats/min (bpm) and the electrical field stimulation (EFS) was applied in conjunction with the pacing stimulation. Isoproterenol was perfused for 30 seconds using the indicated doses. For HDAC inhibition, wild type and *not3*$^{+/-}$ mice were treated with vehicle, Trichostatin A (TSA) or Valproic acid (VPA) for 1 week. Acid-extracted histones were prepared, resolved, and transferred to nitrocellulose membranes for Western blotting. Transverse aorta constriction (TAC) was performed as described (Kuba et al., 2007). For heart

histology, hearts were arrested, fixed, embedded in paraffin and stained with hematoxylin and eosin (H&E) or Masson-Trichrome.

Human QT interval association

Human QT interval association signals over the NOT3 region were obtained from data generated by the QTSCD Consortium (Pfeufer et al., 2009).

Supplementary Material

Refer to Web version on PubMed Central for supplementary material.

Acknowledgments

We thank all members of our laboratories and the VDRC, the BERC (Akita University), and Vincent Chen for helpful discussions and excellent technical support. We thank Eric Olson for the Hand-Gal4 driver and Manfred Frasch for TinCΔ4-Gal4 driver stocks. We thank the members of the QTSCD consortium for valuable support and discussion. JMP is supported by IMBA, the Austrian Ministry of Science, an ERC Advanced Investigator grant, and EuGeneHeart. KK is supported by Kaken (21659198) from Japanese Ministry of Science, MTT Program, and Japan Heart Foundation. GGN was supported by a Marie Curie International Incoming Fellowship. AC was supported by a postdoctoral fellowship and KO by a Scientist Development Grant from the American Heart Association. RB was supported by grants from NHLBI of NIH. AP is supported by grants 01GR0803 and 01EZ0874 from the German federal ministry of research (BMBF), FSID-261/2008 from the The UK Foundation for the Study of Infant Deaths (FSID) and YGEIA/1104/17 and ERYEX/0406/06 from the Cyprus Cardiovascular disease Educational and Research Trust (CCDERT). YI is supported by Global COE program.

References

A.H.A. 2005. http://www.americanheart.org/

Alayari NN, Vogler G, Taghli-Lamallem O, Ocorr K, Bodmer R, Cammarato A. Fluorescent Labeling of *Drosophila* Heart Structures. J Vis Exp. 2009

Albert TK, Lemaire M, van Berkum NL, Gentz R, Collart MA, Timmers HT. Isolation and characterization of human orthologs of yeast CCR4-NOT complex subunits. Nucleic acids research 2000;28:809–817. [PubMed: 10637334]

Behm-Ansmant I, Rehwinkel J, Doerks T, Stark A, Bork P, Izaurralde E. mRNA degradation by miRNAs and GW182 requires both CCR4:NOT deadenylase and DCP1:DCP2 decapping complexes. Genes & development 2006;20:1885–1898. [PubMed: 16815998]

Bodmer R. Heart development in Drosophila and its relationship to vertebrates Trends in cardiovascular medicine. 1995;5:21–28.

Cripps RM, Olson EN. Control of cardiac development by an evolutionarily conserved transcriptional network. Developmental biology 2002;246:14–28. [PubMed: 12027431]

Denis CL. Identification of new genes involved in the regulation of yeast alcohol dehydrogenase II. Genetics 1984;108:833–844. [PubMed: 6392016]

Dietzl G, Chen D, Schnorrer F, Su KC, Barinova Y, Fellner M, Gasser B, Kinsey K, Oppel S, Scheiblauer S, et al. A genome-wide transgenic RNAi library for conditional gene inactivation in Drosophila. Nature 2007;448:151–156. [PubMed: 17625558]

Dudbridge F, Gusnanto A. Estimation of significance thresholds for genomewide association scans. Genetic epidemiology 2008;32:227–234. [PubMed: 18300295]

Fink M, Callol-Massot C, Chu A, Ruiz-Lozano P, Izpisua Belmonte JC, Giles W, Bodmer R, Ocorr K. A new method for detection and quantification of heartbeat parameters in Drosophila, zebrafish, and embryonic mouse hearts. BioTechniques 2009;46:101–113. [PubMed: 19317655]

Gordon T, Castelli WP, Hjortland MC, Kannel WB, Dawber TR. Predicting coronary heart disease in middle-aged and older persons. The Framington study. Jama 1977;238:497–499. [PubMed: 577575]

Han Z, Olson EN. Hand is a direct target of Tinman and GATA factors during Drosophila cardiogenesis and hematopoiesis. Development (Cambridge, England) 2005;132:3525–3536.

Hu G, Kim J, Xu Q, Leng Y, Orkin SH, Elledge SJ. A genome-wide RNAi screen identifies a new transcriptional module required for self-renewal. Genes & development 2009;23:837–848. [PubMed: 19339689]

Jayne S, Zwartjes CG, van Schaik FM, Timmers HT. Involvement of the SMRT/NCoR-HDAC3 complex in transcriptional repression by the CNOT2 subunit of the human Ccr4-Not complex. The Biochemical journal 2006;398:461–467. [PubMed: 16712523]

Joza N, Oudit GY, Brown D, Benit P, Kassiri Z, Vahsen N, Benoit L, Patel MM, Nowikovsky K, Vassault A, et al. Muscle-specific loss of apoptosis-inducing factor leads to mitochondrial dysfunction, skeletal muscle atrophy, and dilated cardiomyopathy. Molecular and cellular biology 2005;25:10261–10272. [PubMed: 16287843]

Kuba K, Zhang L, Imai Y, Arab S, Chen M, Maekawa Y, Leschnik M, Leibbrandt A, Markovic M, Schwaighofer J, et al. Impaired heart contractility in Apelin gene-deficient mice associated with aging and pressure overload. Circulation research 2007;101:e32–42. [PubMed: 17673668]

Lakatta EG, Levy D. Arterial and cardiac aging: major shareholders in cardiovascular disease enterprises: Part II: the aging heart in health: links to heart disease. Circulation 2003;107:346–354. [PubMed: 12538439]

Laribee RN, Shibata Y, Mersman DP, Collins SR, Kemmeren P, Roguev A, Weissman JS, Briggs SD, Krogan NJ, Strahl BD. CCR4/NOT complex associates with the proteasome and regulates histone methylation. Proceedings of the National Academy of Sciences of the United States of America 2007;104:5836–5841. [PubMed: 17389396]

Lloyd-Jones D, Adams R, Carnethon M, De Simone G, Ferguson TB, Flegal K, Ford E, Furie K, Go A, Greenlund K, et al. Heart disease and stroke statistics--2009 update: a report from the American Heart Association Statistics Committee and Stroke Statistics Subcommittee. Circulation 2009;119:e21–181. [PubMed: 19075105]

Lo PC, Frasch M. A role for the COUP-TF-related gene seven-up in the diversification of cardioblast identities in the dorsal vessel of Drosophila. Mechanisms of development 2001;104:49–60. [PubMed: 11404079]

Morita H, Seidman J, Seidman CE. Genetic causes of human heart failure. The Journal of clinical investigation 2005;115:518–526. [PubMed: 15765133]

Moss AJ, Kass RS. Long QT syndrome: from channels to cardiac arrhythmias. The Journal of clinical investigation 2005;115:2018–2024. [PubMed: 16075042]

Mudd JO, Kass DA. Tackling heart failure in the twenty-first century. Nature 2008;451:919–928. [PubMed: 18288181]

Nabel EG. Cardiovascular disease. The New England journal of medicine 2003;349:60–72. [PubMed: 12840094]

Nerbonne JM. Studying cardiac arrhythmias in the mouse--a reasonable model for probing mechanisms? Trends in cardiovascular medicine 2004;14:83–93. [PubMed: 15121155]

Ocorr K, Perrin L, Lim HY, Qian L, Wu X, Bodmer R. Genetic control of heart function and aging in Drosophila. Trends in cardiovascular medicine 2007a;17:177–182. [PubMed: 17574126]

Ocorr K, Reeves NL, Wessells RJ, Fink M, Chen HS, Akasaka T, Yasuda S, Metzger JM, Giles W, Posakony JW, et al. KCNQ potassium channel mutations cause cardiac arrhythmias in Drosophila that mimic the effects of aging. Proceedings of the National Academy of Sciences of the United States of America 2007b;104:3943–3948. [PubMed: 17360457]

Paternostro G, Vignola C, Bartsch DU, Omens JH, McCulloch AD, Reed JC. Age-associated cardiac dysfunction in Drosophila melanogaster. Circulation research 2001;88:1053–1058. [PubMed: 11375275]

Peng W, Togawa C, Zhang K, Kurdistani SK. Regulators of cellular levels of histone acetylation in Saccharomyces cerevisiae. Genetics 2008;179:277–289. [PubMed: 18493053]

Pfeufer A, Sanna S, Arking DE, Muller M, Gateva V, Fuchsberger C, Ehret GB, Orru M, Pattaro C, Kottgen A, et al. Common variants at ten loci modulate the QT interval duration in the QTSCD Study. Nature genetics 2009;41:407–414. [PubMed: 19305409]

Qian L, Bodmer R. Partial loss of GATA factor Pannier impairs adult heart function in Drosophila. Human molecular genetics 2009;18:3153–3163. [PubMed: 19494035]

Qian L, Mohapatra B, Akasaka T, Liu J, Ocorr K, Towbin JA, Bodmer R. Transcription factor neuromancer/TBX20 is required for cardiac function in Drosophila with implications for human heart disease. Proceedings of the National Academy of Sciences of the United States of America 2008;105:19833–19838. [PubMed: 19074289]

Ray VM, Dowse HB. Mutations in and deletions of the Ca2+ channel-encoding gene cacophony, which affect courtship song in Drosophila, have novel effects on heartbeating. Journal of neurogenetics 2005;19:39–56. [PubMed: 16076631]

Rusconi JC, Challa U. Drosophila Mrityu encodes a BTB/POZ domain-containing protein and is expressed dynamically during development. The International journal of developmental biology 2007;51:259–263. [PubMed: 17486548]

Sanguinetti MC, Tristani-Firouzi M. hERG potassium channels and cardiac arrhythmia. Nature 2006;440:463–469. [PubMed: 16554806]

Sanyal S, Jennings T, Dowse H, Ramaswami M. Conditional mutations in SERCA, the Sarco-endoplasmic reticulum Ca2+-ATPase, alter heart rate and rhythmicity in Drosophila. Journal of comparative physiology 2006;176:253–263.

Tucker M, Valencia-Sanchez MA, Staples RR, Chen J, Denis CL, Parker R. The transcription factor associated Ccr4 and Caf1 proteins are components of the major cytoplasmic mRNA deadenylase in Saccharomyces cerevisiae. Cell 2001;104:377–386. [PubMed: 11239395]

Wang Q, Curran ME, Splawski I, Burn TC, Millholland JM, VanRaay TJ, Shen J, Timothy KW, Vincent GM, de Jager T, et al. Positional cloning of a novel potassium channel gene: KVLQT1 mutations cause cardiac arrhythmias. Nature genetics 1996;12:17–23. [PubMed: 8528244]

Yusuf S, Reddy S, Ounpuu S, Anand S. Global burden of cardiovascular diseases: part I: general considerations, the epidemiologic transition, risk factors, and impact of urbanization. Circulation 2001;104:2746–2753. [PubMed: 11723030]

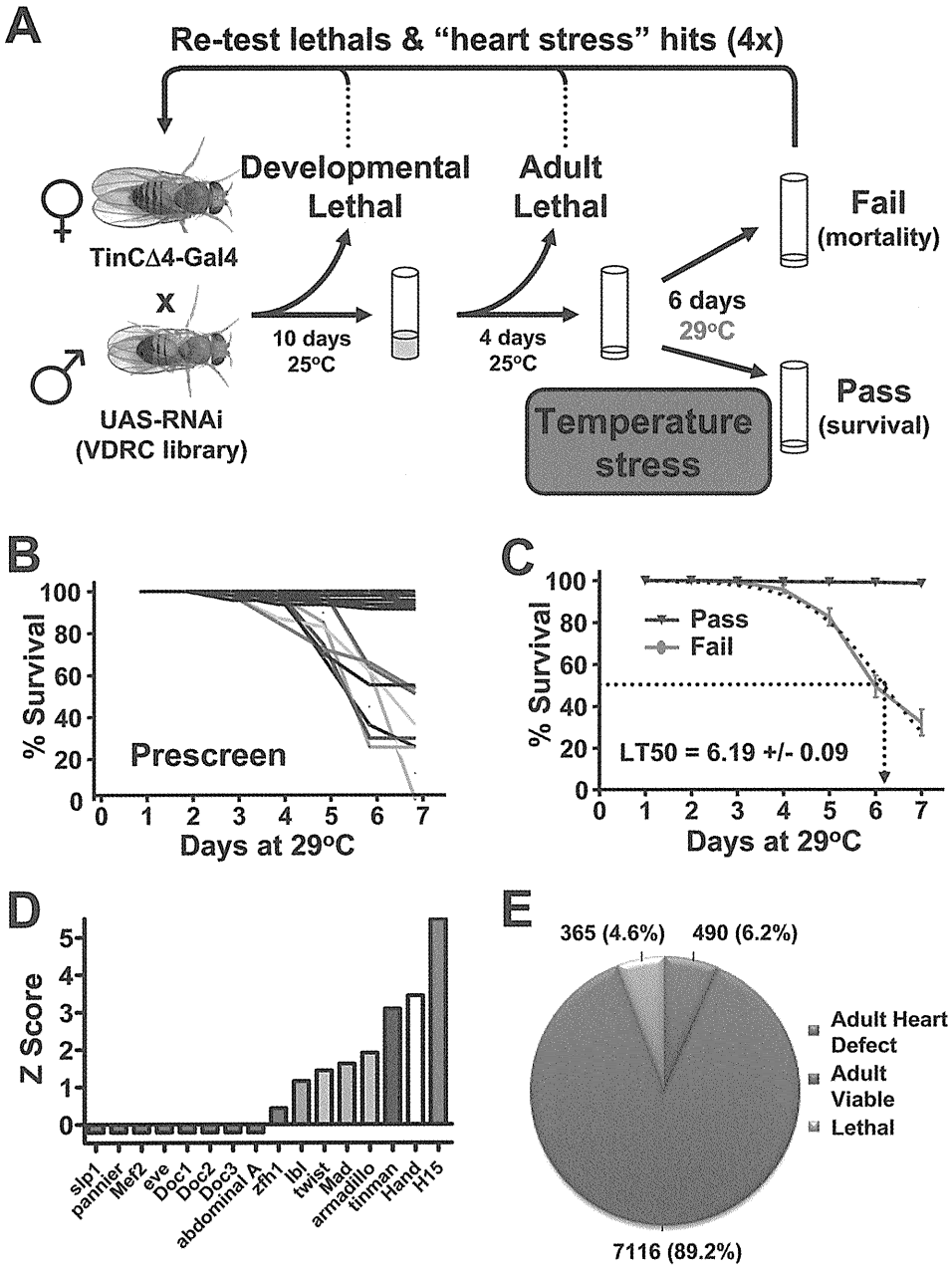

Figure 1. Genome wide screen for conserved heart genes

(A) Schematic for screen setup. TinΔ4-Gal4, a cardiac tissue specific driver, was used to drive conserved UAS-RNAi hairpins in the developing heart. Developmental lethality and baseline adult viability was scored. Viable adult flies were then given a heart stress (continued exposure to 29°C) and survival was scored on day 6. Fly lines showing a potential developmental or heart function phenotype were then retested to confirm the candidate gene. **(B)** 80 randomly selected UAS-RNAi lines were crossed to TinCΔ4-Gal4 and evaluated for adult lethality following an increase in ambient temperate as cardiac stressor. Lines were either viable (black) or died starting around day 3. Data from individual lines are shown as % survival on the indicated days. **(C)** Mean responses from viable and failing (death after exposure to 29°C) flies

revealed an average lethal time at which 50% of failing flies died (LT50) of 6.19 days. **(D)** Efficacy of TinCΔ4-Gal4 x UAS-RNAi lines to knock-down transcription factors known to play a role in heart formation. **(E)** Using this system a genome-wide screen was performed to search for conserved candidate genes for adult heart function under conditions of cardiac stress. 4.6% TinCΔ4-Gal4 x UAS-RNAi lines were developmental lethal. Among the 7971 viable lines, 490 transformant lines exhibited significantly increased death (Z-score >3, determined on day 6 after shifting the ambient temperature to 29°C). See also Figure S1 and Tables S1 and S2.

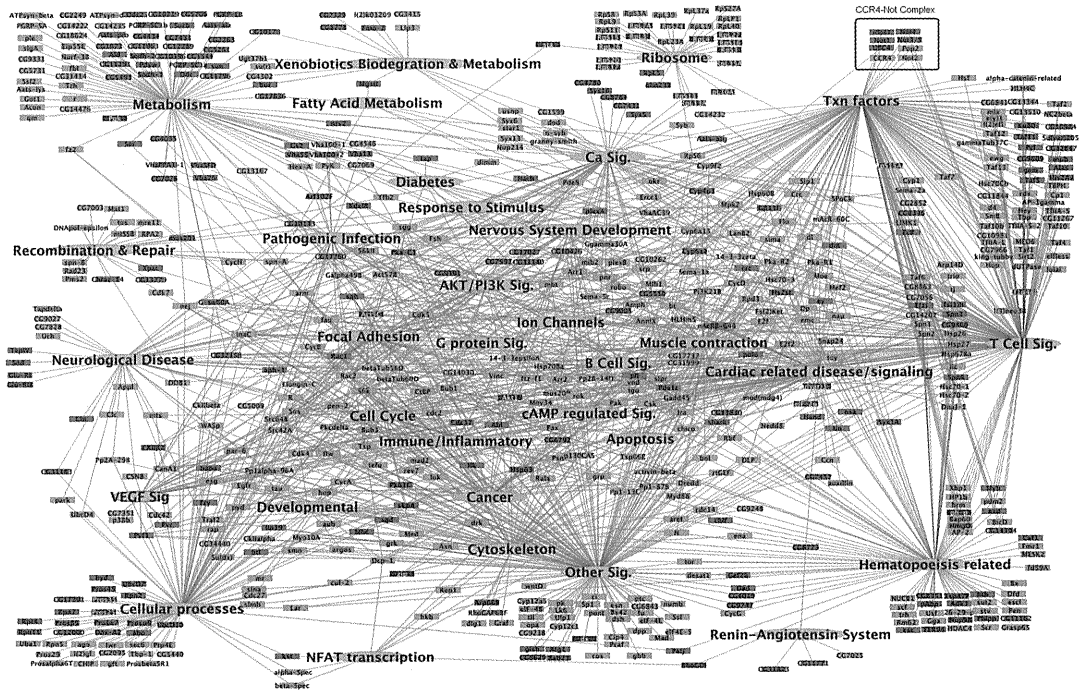

Figure 2. A global network of heart function

The systems network includes data from the significantly enriched *Drosophila* KEGG and mouse and human KEGG and C2 data sets. Pathways and gene sets from the same biological processes were grouped into common functional categories. Green nodes represent statistically enriched functional categories of pathways; red nodes represent direct primary fly RNAi hits; light red nodes represent their first degree binding partners; and blue nodes indicate genes that were scored as developmentally lethal in our *Drosophila* heart screen. Lines indicate associations of the genes to the appropriate functional category. All KEGG pathways and selected C2 gene sets have been represented in the systems map. See also Tables S3–S5.

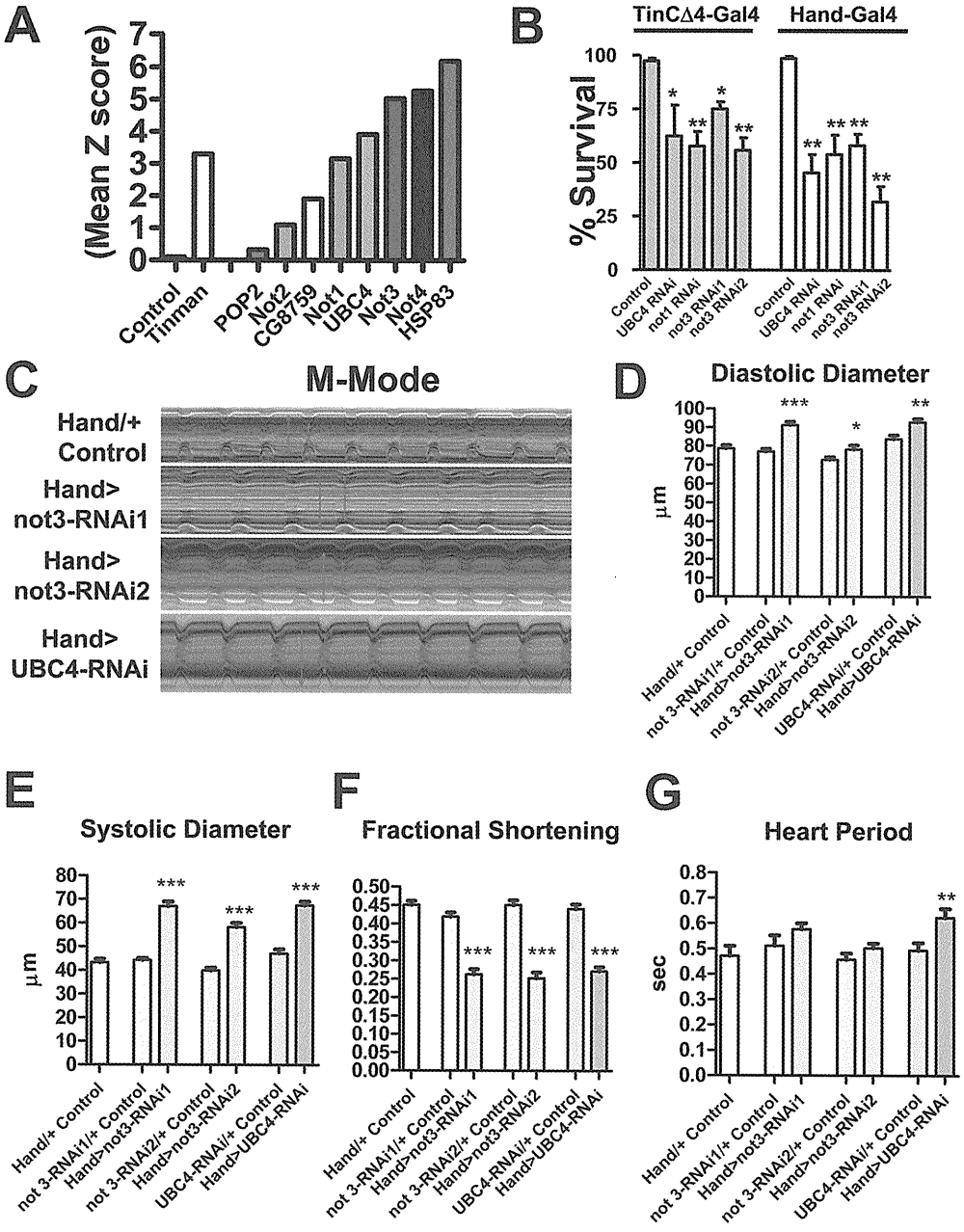

Figure 3. The CCR4-Not complex is a central regulator of adult heart function and loss of not3 results in dilated cardiomyopathy in *Drosophila*

(A) Mean Z scores for TinCΔ4-Gal4 x UAS-RNAi lines targeting the indicated members of the fly CCR4-Not complex. A negative control (w^{1118} [isogenic to the RNAi library] X TinΔ4-Gal4) and the positive control Tinman RNAi line are shown. **(B)** Not1, not3, and UBC4 are essential for proper adult heart function in both Tinman and Hand-expressing cells. Data are shown as mean +/− SEM for at least 3 replicates. RNAi1 and RNAi2 indicate different transgenic hairpins targeting *not3*. * $p<0.05$, ** $p<0.01$ by ANOVA. **(C)** 1 week old adult flies with Hand-Gal4 driving not3 or UBC4 cardiac specific knock-down exhibit impaired heart function. M-modes provide traces of the heart contractions to document the movements in a 1

pixel-wide region of the heart tube over time. HandG4/+ control are the progeny of Hand-Gal4 crossed to w^{1118}. Hand>Not3-RNAi are the progeny of Hand-Gal4 crossed to either UAS-*not3*-RNAi (−1 or −2) or UAS-*UBC4*-RNAi lines. Fly heart analysis was generated using a MatLab based image analysis program (Fink et al., 2009; Ocorr et al., 2007b). M-modes of the RNAi knockdown hearts reveal dilated diastolic and systolic diameters (double-headed red arrows) and reduced shortening properties (difference between diameters) when compared to M-modes of control hearts. Each trace represents a 5 second recording. **(D–G)** *Not3* or *UBC4* heart specific knock-down perturbs several indices of cardiac performance. Progeny of Hand-Gal4 crossed to two different *UAS-not3*-RNAi lines or an *UAS-UBC4*-RNAi line (experimental), and w^{1118} crossed to UAS-RNAi or Hand-Gal4 driver (controls) were used for these experiments as in C. *not3* and *UBC4* knockdown led to significantly wider **(D)** diastolic and **(E)** systolic diameters, and as a result significantly depressed **(F)** fractional shortening in all experimental lines relative to controls. **(G)** *not3* knockdown trended toward a slight lengthening in the heart period (time between consecutive diastolic intervals) while *UBC4* knockdown led to a significant increase in heart period. Mean values ± SEM are shown for each group (n = 29–40). Unpaired t-tests were performed between each Hand-Gal4>UAS-RNAi and each corresponding UAS-RNAi/+ control (progeny of w^{1118} crossed to UAS-RNAi line). Additionally, one-way ANOVAs with Bonferroni multiple comparison tests revealed no significant differences between the HandG4/+ control and all UAS-RNAi/+ control lines, for any cardiac parameter measured. * $p<0.05$, ** $p<0.01$, *** $p<0.001$. See also Figure S3 and Video S1.

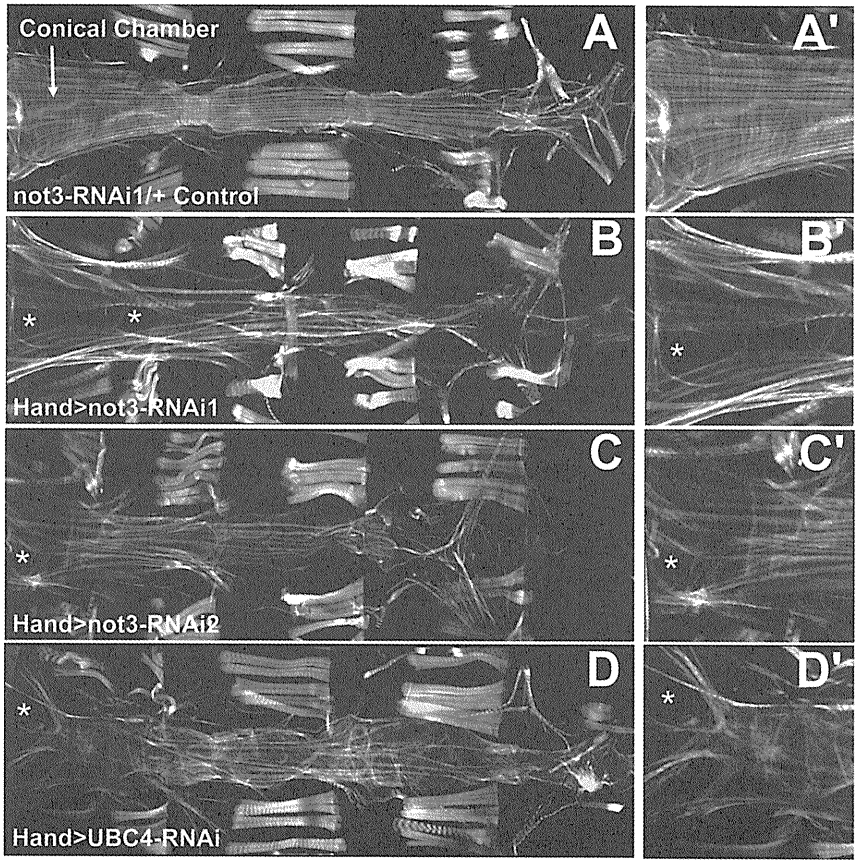

Figure 4. *not3* and *UBC4* cardiac specific RNAi-knockdown substantially perturb myofibrillar organization and content

(A) Alexa584-phalloidin staining of control *Drosophila* cardiac tubes reveals typical spiraling myofibrillar arrangements within the cardiomyocytes. The fibers, especially those in the conical chamber, located anteriorly, are densely packed with f-actin. **(B–D)** Relative to control hearts, *not3* or *UBC4* RNAi knockdown severely disrupts myofibrillar organization and leads to an apparent loss of myofilaments as noted by large gaps in f-actin staining (*) as well as by a lack of myosin heavy chain transcripts (Fig. S4F). **(A′-D′)** Enlarged images of the conical chambers from **A–D,** respectively, which illustrate the high degree of myofibrillar disarray and large gaps in f-actin staining within the cardiomyocytes of *not3* and *UBC4* RNAi knockdown hearts. Original images taken at 10X magnification with a Zeiss Imager Z1 fluorescent microscope.

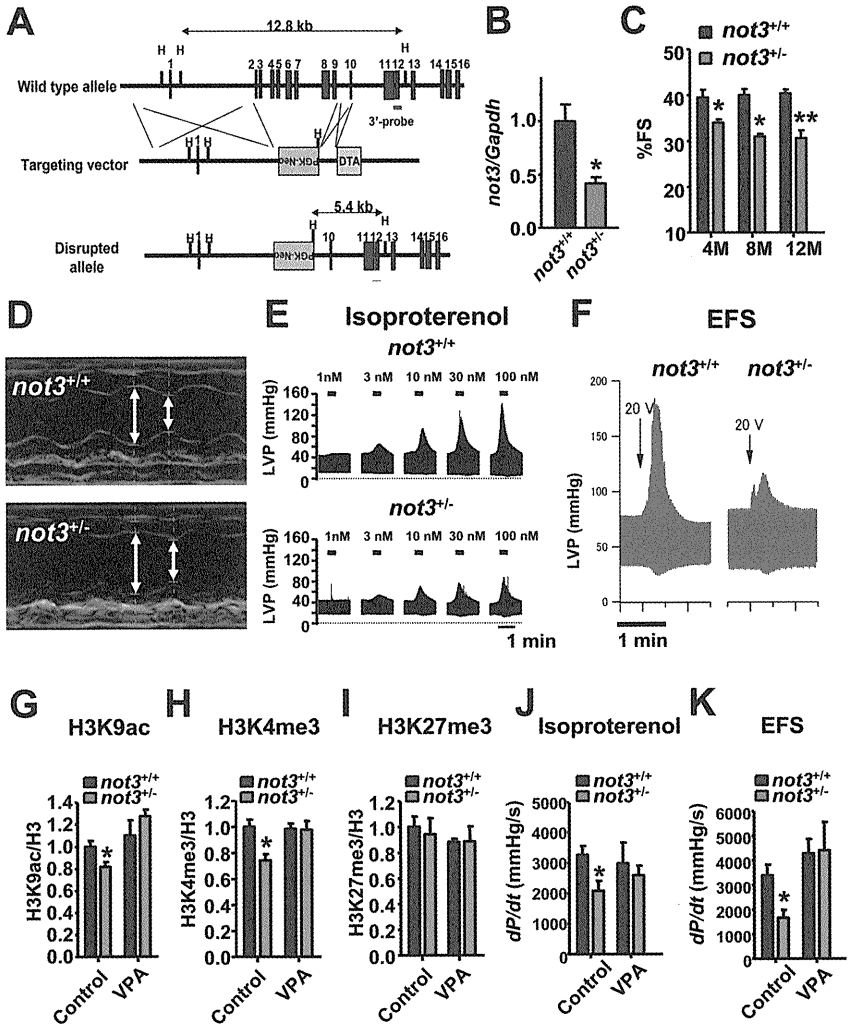

Figure 5. *not3*$^{+/-}$ mice exhibit reduced heart contractility, *ex vivo* function, and histone modifications that can be rescued by treatment with HDAC inhibitors

(A) Gene targeting strategy. Exons 2 to 9 of the *not3* gene (official symbol *cnot3*) were replaced with a PGK-Neo cassette by homologous recombination in A9 ES cells. The wild type allele, the targeting vector, and mutant allele, and the PGK-Neo and DTH selection cassettes are shown. Blue boxes indicate exons. **(B)** Real-time PCR analyses for *not3* mRNA expression in 3 month old wild-type and *not3*$^{+/-}$ hearts. Values were normalized to *gapdh* mRNA expression. n = 6 mice per group. **(C)** *not3*$^{+/-}$ mice display a significant reduction in % fractional shortening at 4 months of age, which became more pronounced with age. n = 6–8 mice per group. Fractional shortening was determined by echocardiography. **(D)** Representative M-mode echocardiography for wild-type and *not3*$^{+/-}$ mice at 8 months of age. **(E)** Left ventricular pressure (LVP) measurements in isolated *ex vivo not3*$^{+/-}$ and *not3*$^{+/+}$ hearts under isoproterenol perfusion. *not3*$^{+/-}$ hearts from 4 months old mice showed impaired contractile responses to different doses of isoproterenol perfusion in the retrograde Langendorff mode as compared to age matched controls. **(F)** Impaired contractile response of *ex vivo not3*$^{+/-}$ hearts to electrical field stimulation (EFS) compared with littermate *not3*$^{+/+}$ hearts. Representative data for left ventricular pressure (LVP) at 20V stimulation are shown. **(G)** H3K9 acetylation (H3K9ac), **(H)** H3K4 trimethylation (H3K4me3) and **(I)** H3K27 trimethylation (H3K27me3) levels were

analyzed by Western blot for acid-extracted histones from whole heart ventricles of wild type and *not3*$^{+/-}$ mice treated with vehicle or VPA (0.71% w/v in drinking water for 1 week) Band intensities were normalized to total H3 levels. **(J** and **K)** Treatment (1 week) with the HDAC inhibitor VPA rescue impaired *ex vivo* heart contractility of *not3*$^{+/-}$ hearts to isoproterenol (100nM) perfusion or 25V EFS. All values are mean +/− SEM. *; $P < 0.05$, **; $P < 0.01$. n = 5–12 per group. See also Figure S4 and S5.

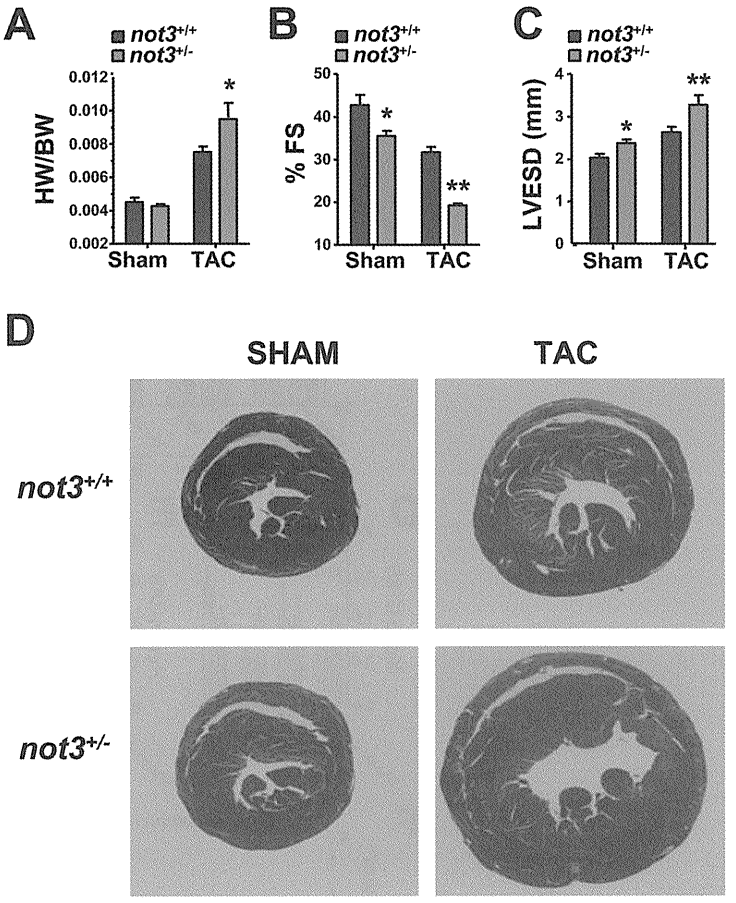

Figure 6. *Not3*$^{+/-}$ mice exhibit severe heart failure in response to pressure overload

(A) Heart weight to body weight ratios (HW/BW) in *not3*$^{+/-}$ and *not3*$^{+/+}$ littermate mice 3 weeks after transverse aortic constriction (TAC). Animals receiving sham surgery are shown as controls. **(B)** and **(C)** Echocardiography of male *not3*$^{+/-}$ and wild type littermates 3 weeks after TAC. *not3*$^{+/-}$ mice with TAC show **(B)** decreased % fractional shortening (%FS) and **(C)** increased left ventricular diameter in systolic phase (LVESD) compared with *not3*$^{+/+}$ mice that received TAC. **(D)** Representative sections of *not3*$^{+/+}$ and *not3*$^{+/-}$ hearts analyzed 3 weeks after sham or TAC surgery. Masson-trichrome staining are shown to visualize collagen deposits indicative of fibrotic changes. Note the severe cardiac hypertrophy and ventricular dilation in *not3*$^{+/-}$ mice following TAC.

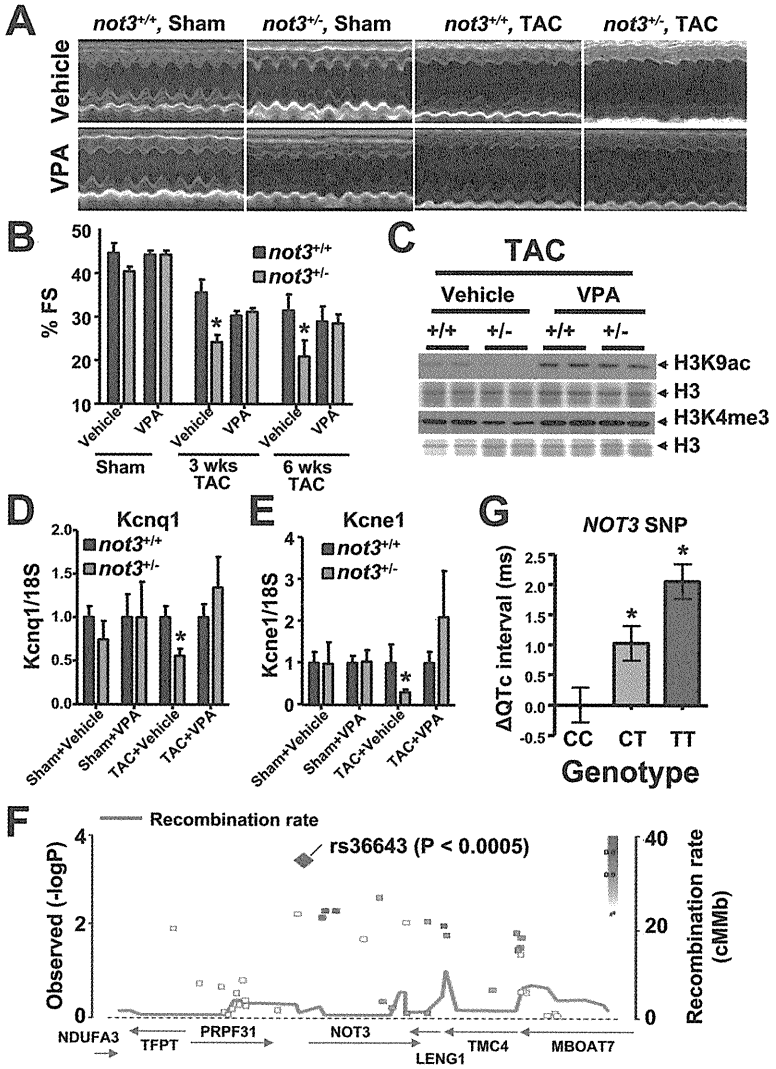

Figure 7. Not3 is a conserved regulator of heart function

(A and **B)** Rescue of severe heart failure in TAC *not3*$^{+/-}$ hearts by the HDAC inhibitor VPA. One day after TAC or sham surgery the mice received treatment with vehicle or VPA (0.71% w/v in drinking water) for 6 weeks. **(A)** Representative M-mode echocardiography and **(B)** % FS in *not3*$^{+/-}$ and *not3*$^{+/+}$ littermate mice 6 weeks after TAC or sham surgery with or without VPA treatment. **(C)** Reduced H3K9 acetylation (H3K9ac) and H3K4 trimethylation (H3K4me3) levels were rescued by VPA treatment. Acid-extracted histones from the hearts 6 weeks after TAC surgery were immunoblotted with antibodies for H3K9ac and H3K4me3. H3 is shown as a loading control. **(D** and **E)** Real time PCR analyses for the QT interval-associated potassium channel genes Kcnq1 and Kcne1. Total RNA was isolated from hearts 6 weeks after TAC or sham surgery with or without VPA treatment, and Kcnq1 and Kcne1 mRNA levels were measured and normalized to 18S mRNA. Data are shown as fold changes compared to *not3*$^{+/+}$ mice for each treatment group. Values are mean +/− SEM. *; $P < 0.05$, **; $P < 0.01$. n = 5–10 per group. **(F)** Regional visualization of the association signal between common variants in the NOT3 region and the adjusted QT interval (QTc). SNP rs36643 in the 5′ region of NOT3 (−969bp from the transcription start and −924 from the TATA box) showed a

significant regional association (p=0.000366). (**G**) Association between the T allele of SNP rs36643 and a prolongation of QTc. * P< 0.0005 from linear regression with inverse variance weighting using an additive genetic model. Data is derived from a meta-analysis of genome-wide association scans in several populations (Pfeufer et al., 2009). See also Figure S6.